

MP-RDMA: Enabling RDMA With Multi-Path Transport in Datacenters

Guo Chen[✉], Yuanwei Lu, Bojie Li[✉], Kun Tan, Yongqiang Xiong, Peng Cheng[✉], Jiansong Zhang, and Thomas Moscibroda

Abstract—RDMA is becoming prevalent because of its low latency, high throughput and low CPU overhead. However, in current datacenters, RDMA remains a single path transport which is prone to failures and falls short to utilize the rich parallel network paths. Unlike previous multi-path approaches, which mainly focus on TCP, this paper presents a multi-path transport for RDMA, *i.e.* MP-RDMA, which efficiently utilizes the rich network paths in datacenters. MP-RDMA employs three novel techniques to address the challenge of limited RDMA NICs on-chip memory size: 1) a *multi-path ACK-clocking* mechanism to distribute traffic in a congestion-aware manner without incurring per-path states; 2) an *out-of-order aware path selection* mechanism to control the level of out-of-order delivered packets, thus minimizes the meta data required to them; 3) a *synchronise* mechanism to ensure in-order memory update whenever needed. With all these techniques, MP-RDMA only adds 66B to each connection state compared to single-path RDMA. Our evaluation with an FPGA-based prototype demonstrates that compared with single-path RDMA, MP-RDMA can significantly improve the robustness under failures ($2\times\sim4\times$ higher throughput under $0.5\%\sim10\%$ link loss ratio) and improve the overall network utilization by up to 47%.

Index Terms—Datacenter networks, RDMA, multi-path transport, hardware-based transport.

I. INTRODUCTION

MODERN datacenter applications require high throughput and low latency networks to meet the increasing demands from customers. Compared with conventional

Manuscript received October 5, 2018; revised July 8, 2019; accepted September 22, 2019; approved by IEEE/ACM TRANSACTIONS ON NETWORKING Editor M. Schapira. Date of publication November 11, 2019; date of current version December 17, 2019. This work was supported in part by the National Natural Science Foundation of China under Grant 6187060280, in part by the Huawei Innovation Research Program, in part by the Tencent Rhino-Bird Open Research Fund, and in part by the Fundamental Research Funds for the Central Universities. The work of G. Chen was supported by the Science and Technology on Parallel and Distributed Processing Laboratory (PDL). The preliminary version of this article was published in the USENIX Symposium on Networked Systems Design and Implementation (NSDI), 2018. (Corresponding author: Guo Chen.)

G. Chen is with the College of Computer Science and Electronic Engineering, Hunan University, Changsha 410000, China (e-mail: guochen@hnu.edu.cn).

Y. Lu is with Tencent, Shenzhen 518057, China (e-mail: yuanweilu@tencent.com).

B. Li and K. Tan are with the Central Software Institute, Huawei Technologies, Beijing 100036, China (e-mail: libojie2@huawei.com; kun.tan@huawei.com).

Y. Xiong and P. Cheng are with Microsoft Research Asia, Beijing 100080, China (e-mail: yqx@microsoft.com; pengc@microsoft.com).

J. Zhang is with Alibaba, Beijing 100000, China (e-mail: jiansongzhang@live.com).

T. Moscibroda is with Microsoft Azure, Seattle, WA 98007 USA (e-mail: moscitho@microsoft.com).

Digital Object Identifier 10.1109/TNET.2019.2948917

software transport, Remote Direct Memory Access (RDMA) implements the entire transport logic in hardware network interface card (NIC) and allows direct access to remote memory, mostly bypassing CPU. Therefore, RDMA provides ultra-low latency ($\sim 1\mu s$) and high throughput (40/100Gbps) with little CPU overhead. Nowadays, RDMA has been deployed in datacenters at scale with RDMA over Converged Ethernet (RoCE) v2 [2], [3]. Existing RDMA is a single path transport, *i.e.*, an RDMA connection only flows along one network path¹. This single path transport is prone to path failures and also cannot utilize the rich parallel paths in modern datacenters [5]–[7]. While many approaches have been proposed to enhance TCP to support multi-path, none has considered RDMA. In this paper, we propose a multi-path transport for RDMA.

However, RDMA is completely implemented in NIC hardware which has very limited computing resource and on-chip memory (*e.g.*, only a few mega-bytes). Although NIC could upload local states in host memory, swapping data between on-chip memory and host memory has a cost and frequent swapping would significantly downgrades performance [8], [9] (also see §II-C). As a consequence, the key design goal for a multi-path RDMA transport is to minimize the memory footprint, which incurs three challenges.

First, a multi-path transport should track the congestion states on each path, so that it can perform congestion-aware load distribution. However, these states grow linearly with the number of sending paths. This may cause a considerable memory overhead even when a modest number of paths are used for one RDMA connection. For example, if we adopt a multi-path transport similar to MPTCP [5], we may add 368 bytes if 8 sub-flows are used.² However, the size of these extra states is already $\sim 50\%$ more than the entire states of one connection in current RoCE design.³ As a result, significantly fewer concurrent connections can be supported only using on-chip memory, which leads to more frequent swapping and downgrades the performance.

Second, multi-path will cause packets to arrive out-of-order at the receiver. Consequently, the receiver needs additional metadata to track whether a packet has arrived or not. However, if the paths conditions vary greatly, the size of the metadata could be large. Fig. 1 gives the 99.9% tail of

¹In this paper, RDMA refers to RoCEv2 which is widely used in datacenters. We note that RDMA in high-performance computing (*i.e.*, InfiniBand RDMA) has multi-path solutions [4]. However, the InfiniBand underlying network is totally different from the datacenter Ethernet network. This paper aims to design a multi-path transport for RDMA in datacenters (*i.e.*, RoCEv2).

²Each sub-connection needs to maintain states including *recv_nxt*, *snd_nxt*, *snd_una*, *snd_ssthresh*, *snd_cwnd*, *srtt*, *rttvar*, *rtt_seq*, *map_data_seq*, *map_subseq*, *map_data_len*, ...

³Mellanox ConnectX Linux driver [10] maintains all the states of an RDMA connection in a 256B *mlx4_qp_context*.

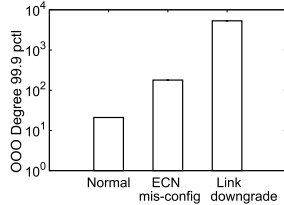


Fig. 1. Out-of-order degree under different scenarios.

the out-of-order degree (OOD)⁴ of a network under various scenarios (more details in § VI-B.1). For example, consider the case that one path has degraded to 1Gbps (*e.g.*, due to hardware failures caused link rate auto-negotiation [6], [11]), while other paths remain at a normal speed of 40Gbps. If a bitmap structure is used, the size of the bitmap would be 1.2KB. If we naively use fewer bits, any packet with a sequence number out of the range of the bitmap has to be dropped. This would reduce the performance greatly as the throughput is effectively limited by the slowest path. A core design challenge is to keep high performance even if we can only track very limited out-of-order packets.

Finally, the receiver NIC does not have enough memory to buffer out-of-order packets but has to place them into host memory as they arrive. Therefore, the data in host memory may be updated out-of-order. This may cause a subtle issue as some existing applications implicitly assume the memory is updated in the same order as the operations are posted [12]–[14]. For example, a process may use a WRITE operation to update a remote memory, and then issues another WRITE operation to set a dirty flag to notify a remote process. If the second WRITE updates memory before the first WRITE, the remote process may prematurely read the partial data and fails. While retaining the memory updating order is trivial for single-path RDMA, it requires careful design in multi-path RDMA to avoid performance downgrade.

This paper presents MP-RDMA, the first multi-path transport for RDMA that addresses all aforementioned challenges. Specifically, MP-RDMA employs a novel *multi-path ACK-clocking* mechanism that can effectively do congestion-aware packets distribution to multiple paths without adding per-path states. Second, we design an *out-of-order aware path selection algorithm* that proactively prunes slow paths and adaptively chooses a set of paths that are fast and with similar delays. This way, MP-RDMA effectively controls the out-of-order level so that almost all packets can be tracked with a small sized bitmap (*e.g.*, 64 bits). Finally, MP-RDMA provides an interface for programmers to ensure in-order memory update by specifying a *synchronise* flag to an operation. A synchronise operation updates memory only when all previous operations are completed. Therefore, two communication nodes can coordinate their behaviors and ensure application logic correctness.

We have implemented an MP-RDMA prototype in FPGA, which can run at the line rate of 40Gbps. We evaluate MP-RDMA in a testbed with 10 servers and 6 switches. Results show that MP-RDMA can greatly improve the robustness under path failures ($2\times\sim4\times$ higher throughput when links have 0.5%~10% loss rate), overall network utilization ($\sim47\%$ higher overall throughput) and average flow

⁴We define the *out-of-order degree (OOD)* here as the maximal difference between the sequence number of an out-of-order arrived packet and the expected packet sequence number.

completion time (up to 17.7% reduction) compared with single-path RDMA. Moreover, MP-RDMA only consumes a small constant (66B) amount of extra per-connection memory, which is comparable to the overhead ($\sim60B$) added by DCQCN [2] to enhance existing single-path RDMA.

In summary, we make the following contributions: 1) We present MP-RDMA, the first transport for RDMA that supports multi-path. 2) We have designed a set of novel algorithms to minimize the memory footprint, so that MP-RDMA is suitable to be implemented in NIC hardware. 3) We have evaluated MP-RDMA on an FPGA-based testbed as well as large-scale simulations.

II. BACKGROUND AND MOTIVATION

A. RDMA Background

RDMA enables direct memory access to a remote system through NIC hardware, by *implementing the transport entirely in NIC*. Therefore RDMA can provide low latency and high throughput with little CPU involvement on either local or remote end. RoCE v2 [15]–[17] introduces UDP/IP/Ethernet encapsulation which allows RDMA to run over generic IP networks. Nowadays, production datacenters, *e.g.* Microsoft Azure and Google, have deployed RoCE at scale [2], [3], [18]. Hereafter in this paper, unless explicitly stated otherwise, we refer RDMA to RoCE v2.

In RDMA terminology, an RDMA connection is identified by a pair of work queues, called *queue pair* (QP). A QP consists of a *send* queue and a *receive* queue which are both maintained on NICs. When an application initiates an RDMA *operation* (also called a *verb*) to send or retrieve data, it will post a *work queue element* (WQE) to NIC's send queue or receive queue, respectively. Moreover, to notify the application for operation completion, there is also a completion queue (CQ) associated with each QP. On completing a WQE, a completion queue element (CQE) will be delivered to the CQ. There are four commonly used verbs in RDMA: SEND, RECV, WRITE and READ. Among these, SEND and RECV are *two-sided*, meaning that SEND operation always requires a RECV operation at the other side. READ and WRITE are *one-sided* operations, meaning that applications can directly READ or WRITE pre-registered remote memory without involving remote CPU.

RDMA transport is message-based, *i.e.* an RDMA operation is translated into a *message* for transmission. Then an RDMA message will be divided into multiple equal-sized *segments* which are encapsulated into UDP/IP/Ethernet packet(s). In RoCEv2, all RDMA packets use an identical UDP destination port (4791), while the UDP source port is arbitrary and varies for different connections, which allows load-balancing. An RDMA header is attached to every packet. The header contains a *packet sequence number* (PSN) which provides a continuous sequence number for the RDMA packets in a connection. At the receiver side, RDMA messages are restored according to PSN. Moreover, an RDMA receiver may generate an ACK or a Negative ACK (NACK) to notify the sender for received or lost packets.

RDMA is often deployed on top of a lossless network provided by priority-based flow control (PFC) [19], [20]. Specifically, PFC employs a hop-by-hop flow control on traffic with pre-configured priorities. With PFC, when a downstream switch detects that an input queue exceeds a threshold, it will send a PAUSE frame back to the upstream switch. While PFC

can effectively prevent switches from dropping packets, the back-pressure behavior may propagate congestion and slow down the entire network. Thus, end-to-end congestion control mechanisms have been introduced into RoCE. For example, DCQCN [2] enhances RoCE transport with explicit congestion notification (ECN) and quantized congestion notification (QCN) [21] to control congestion.

B. Need for Multi-Path Transmission

Current RDMA transport mandates a connection to follow one network path. Specifically, packets of one RDMA connection use the same UDP source and destination ports. There are two major drawbacks for such single-path transmission.

First, single path transmission is prone to path failures. Some minor failures along the path can greatly affect the performance of upper-layer applications. For example, silent packet loss is a common failure in datacenter [11], [22]. Since RDMA transport is implemented in hardware which typically lacks resources to realize sophisticated loss recovery mechanism, it is very sensitive to packet loss. As a result, a small loss rate (*e.g.*, 0.1%) along the transmission path can lead to dramatic RDMA throughput degradation (*e.g.*, <~60%) [2].

Second, single path falls short to utilize the overall network bandwidth. Equal Cost Multi-Path (ECMP) routing is currently the main [3], [23], [24] method to balance RDMA traffic among the datacenter network fabrics. Basically, ECMP hashes different connections to different paths. However, as many prior studies pointed out [3], [25], ECMP is not able to balance traffic well when the number of parallel paths is large [26], [27] due to hash collisions. While some part of the network is highly congested, the rest may often have a low traffic load, reducing the overall network utilization. Therefore, it is important to spread traffic in finer granularity than flow among multiple paths to achieve high network utilization [5], [25].

In literature, a set of mechanisms have been proposed to distribute traffic in finer-grained ways to efficiently utilize the rich network paths in datacenters [5]–[7], [25], [28]–[33]. Unfortunately, most of these previous arts only consider TCP traffic, and none of them explicitly discuss RDMA (see §VII for more discussions). As we will show in §II-C, RDMA is quite different from TCP in many aspects. Therefore, in this paper, we design the first multi-path transport for RDMA.

C. Challenges for Multi-Path RDMA

RDMA is implemented in NICs. But usually, on-chip memory in NIC is small and expensive. Populating large memories in NIC hardware is very costly, since memory blocks require many transistors and may occupy a large die area. Thus NICs usually serve as a cache of host memory to store the connection states. If a cache miss happens, RDMA NIC needs to access the host memory via PCIe. Frequent cache misses lead to NIC throughput degradation due to the PCIe bus latency and the contention on the bandwidth. To illustrate the impact of cache misses on application goodput, we use 4 clients with Mellanox ConnectX 3 Pro NICs to initiate RDMA WRITEs to a single server and measure the total goodput. Fig. 2 shows that when the number of concurrent connections is larger than 256, application goodput would drop sharply. This is because to perform WRITE operations, the receiving NIC needs to access corresponding connection states (QP context). When the number of connections is larger

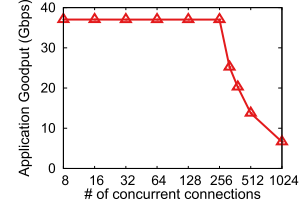


Fig. 2. Goodput of concurrent MLNX CX3 Pro WRITES.

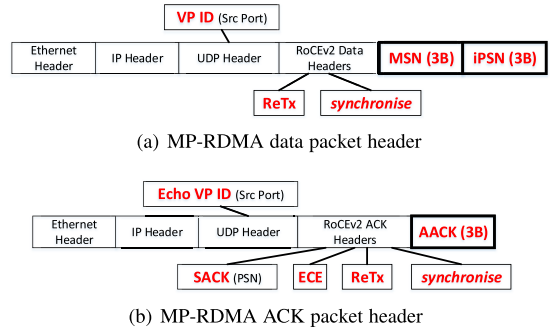


Fig. 3. MP-RDMA packet header format. Fields with red bold text are specific for MP-RDMA.

than 256, not all states can be stored in NIC's memory. With more concurrent connections, cache misses occur more frequently. This result conforms with previous work [8], [9]. Thus, to avoid performance degradation caused by frequent cache misses, the memory footprint for each RDMA connection should be minimized to support more connections in on-chip memory. This key uniqueness of RDMA brings several challenges for designing MP-RDMA as aforementioned (§I).

III. MP-RDMA DESIGN

A. Overview

MP-RDMA is a multi-path transport for RDMA while effectively addresses the challenge of the limited on-chip memory in NIC hardware. MP-RDMA employs a novel ACK-clocking and congestion control mechanism to do congestion-aware load distribution without maintaining per-path states (§III-B). Moreover, it uses an out-of-order aware path selection mechanism to control the out-of-order degree among sending paths, thus minimizes the meta data size required for tracking out-of-order packets (§III-C). Finally, MP-RDMA provides a *synchronise* mechanism for applications to ensure in order host memory update without sacrificing throughput (§III-D).

MP-RDMA assumes a PFC enabled network with RED [34] ECN marking supported. It reuses most of the existing/reserved fields (with thin border) in the UDP and RoCE v2 headers. It extends the existing headers by certain fields (with thick border) (Fig. 3). MP-RDMA controls the transmission paths of a packet by selecting a specific source port in the UDP header and let ECMP pick up the actual path. Since packets with the same source port will be mapped to the same network path, we use a UDP source port to identify a network path, which is termed as a *Virtual Path* (VP). Initially, the sender picks a random VP for a data packet. Upon receiving a data packet, the receiver immediately generates an ACK which encodes the same VP ID (Echo VP ID field). The ACK header carries the PSN of the received data packet (SACK field) as well as the accumulative sequence number

at the data receiver (AACK field). ECN signal (ECE field) is also echoed back to the sender.

The data of a received packet is placed directly into host memory. For WRITE and READ operations, the original RDMA header already embeds the address in every data packet, so the receiver can place the data accordingly. But for SEND/RECV operations, additional information is required to determine the data memory placement address. This address is in a corresponding RECV WQE. MP-RDMA embeds a *message sequence number* (MSN) in each SEND data packet to assist the receiver for determining the correct RECV WQE. In addition, an intra-message PSN (iPSN) is also carried in every SEND data packet as an address offset to place the data of a specific packet within a SEND message.

Next, we zoom into each design component and elaborate how they together can achieve high performance with a small MP-RDMA on-chip memory footprint.

B. Multi-Path Congestion Control

As aforementioned, MP-RDMA performs congestion control without maintaining per-path states, thus minimizing on-chip memory footprint. MP-RDMA uses one congestion window for all paths. The congestion control algorithm is based on ECN. MP-RDMA decreases its *cwnd* proportionally to the level of congestion, which is similar to DCTCP [2]. However, unlike DCTCP that estimates the level of congestion by computing an average ECN ratio, MP-RDMA reacts directly upon ACKs. As packets are rarely dropped in an RDMA network, reacting to every ACK would be precise and reliable. Moreover, it is very simple to implement the algorithm in hardware. MP-RDMA adjusts *cwnd* on a per-packet basis:

For each received ACK:

$$cwnd \leftarrow \begin{cases} cwnd + 1/cwnd & \text{if } ECN = 0 \\ cwnd - 1/2 & \text{if } ECN = 1 \end{cases}$$

Note that on receiving an ECN ACK, *cwnd* is decreased by 1/2 segment instead of cutting by half.

MP-RDMA employs a novel algorithm called *multi-path ACK-clocking* to do congestion-aware packets distribution, which also allows each path to adjust its sending rate independently. The mechanism works as follows: *Initially, the sender randomly spreads initial window (IW) wise of packets to IW initial VPs. Then, when an ACK arrives at the sender, after adjusting cwnd, if packets are allowed, they are sent along the VP carried in the ACK.* In §IV, detailed fluid models and simulations show that with per-packet ECN-based congestion control and multi-path ACK clocking, MP-RDMA can effectively balance traffic among all sending paths based on their congestion level, and also control the queue oscillation gracefully. It is worth noting that MP-RDMA requires per-packet ACK, which adds a tiny bandwidth overhead (< 4%) compared to conventional RDMA protocol.

MP-RDMA uses a similar way as TCP NewReno [35] to estimate the *inflight* packets when there are out-of-order packets being selectively acked.⁵ Specifically, we maintain an *inflate* variable, which increases by one for each received ACK. We use *snd_nxt* to denote the PSN of the highest sent

⁵ Alternatively, we could use a sender-side bitmap to track *sacked* packets. But the memory overhead of this bitmap could be large for high-speed networks due to its large BDP. For example, for 100Gbps network with 100μs delay, the size of the bitmap can be as large as 1220 bits.

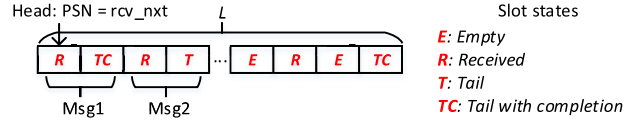


Fig. 4. Data structure to track OOO packets at the receiver.

packet and *snd_una* to denote the PSN of the highest accumulatively acknowledged packet. Then the available window (*awnd*) is:

$$awnd = cwnd + inflate - (snd_nxt - snd_una).$$

Once an ACK moves *snd_una*, *inflate* is decreased by (*ack_aack* − *snd_una*). *ack_aack* denotes the accumulated highest PSN of in-order packets ACKed by the receiver, and *snd_una* will move to the latest *ack_aack* if its AACK field is higher than current *snd_una*. The receiver will generate ACK for each received packet, carrying both the AACK and SACK fields. Note that this estimation can be temporarily inaccurate due to the late arrival of the ACKs with SACK PSN between the old *snd_una* and new *snd_una*. However, the mis-estimation would be compensated once the late SACKs return. Specifically, *inflate* will increase when those SACKs return and the sender will kick out packets for all the under-predicted ACKed packets before. For scenarios that ACKs or packets are lost, MP-RDMA enters retransmission phase and resets *inflate* to zero.

C. Out-of-Order Aware Path Selection

Out-of-Order (OOO) is a common outcome due to the parallelism of multi-path transmission. This section first introduces the data structure for tracking OOO packets. Then we discuss the mechanism to control the network OOO degree to an acceptable level so that the on-chip memory footprint can be minimized.

1) Bitmap to Track Out-of-Order Packets: MP-RDMA employs a simple bitmap data structure at the receiver to track arrived packets. Fig. 4 illustrates the structure of the bitmap, which is organized into a cyclic array. The head of the array refers to the packet with *PSN* = *rcv_nxt*. Each slot contains two bits. According to the message type, a slot can be one of the four states: 1) *Empty*. The corresponding packet is not received. 2) *Received*. The corresponding packet is received, but not the *tail* (last) packet of a message. 3) *Tail*. The packet received is the tail packet of a message. 4) *Tail with completion*. The packet received is the tail packet of a message that requires a completion notification.

When a packet arrives, the receiver will check the PSN in the packet header and find the corresponding slot in the bitmap. If the packet is the tail packet, the receiver will further check the opcode in the packet to see if the message requires a completion notification, *e.g.*, SEND or READ response. If so, the slot is marked as *Tail with completion*; Otherwise, it is marked as *Tail*. For non-tail packets, the slots are simply set to *Received*. The receiver continuously scans the tracking bitmap to check if the head-of-the-line (HoL) message has been completely received, *i.e.*, a continuous block of slots are marked as *Received* with the last slot being either *Tail* or *Tail with completion*. If so, it clears these slots to *Empty* and moves the head point after this HoL message. If the message needs a completion notification, the receiver pops a WQE from the receive WQ and pushes a CQE in the CQ.

2) *Out-of-Order Aware Path Selection*: MP-RDMA employs only limited slots in the tracking bitmap, e.g., $L = 64$, to reduce the memory footprint in NIC hardware. Therefore, if an out-of-order packet holds a PSN larger than $(recv_nxt + L)$, the receiver has to drop this packet, which hurts the overall performance. MP-RDMA controls the degree of out-of-order packets (OOD) by a novel path selection algorithm, so that most packets would arrive within the window of the tracking bitmap. The core idea of our out-of-order aware path selection algorithm is to actively prune the slow paths and select only fast paths with similar delay.

Specifically, we add one new variable, snd_ooh , which records the highest PSN that has been sacked by an ACK. For the sake of description, we define another variable $snd_ool = snd_ooh - \Delta$, where $\Delta \leq L$ is a tunable parameter that determines the out-of-order level of MP-RDMA. The algorithm works as follows: *When an ACK arrives at the sender, the sender will check if the SACK PSN is lower than snd_ool . If so, the sender reduces cwnd by one and this ACK is not allowed to clock out a packet to the VP embedded in the ACK header.*

The design rationale is straightforward. We note that snd_ooh marks an out-of-order packet that goes through the fast path. In order to control the OOD, we need to prune all slow paths that causes an OOD larger than Δ . Clearly, an ACK acknowledges a PSN lower than snd_ool identifies such a slow path with the VP in the header. Note that PSN alone may not correctly reflect the sending order of a retransmitted packet (sent later but with lower PSN). Therefore, to remove this ambiguity, we explicitly tag a bit in packet header to identify a retransmitted packet and echo back in its ACK (ReTx in Fig. 3). For those ReTx ACKs, we simply regard their data packets have used good paths.

New Path Probing: MP-RDMA periodically probes new paths to find better ones. Specifically, every RTT, with a probability p , the sender sends a packet to a new random VP, instead of the VP of the ACK. This p balances the chance to fully utilize the current set of good paths and to find even better paths. In our experiment, we set p to 1%.

D. Handling Synchronise Operations

As discussed in §II, NIC hardware does not have enough memory to store out-of-order packets and has to place them into host memory. One possible way is to allocate a separate re-ordering buffer in host memory and temporarily store the out-of-order packets there. When the HoL message is completely received, the NIC can copy the message from the re-ordering buffer into the right memory location. This, however, causes a significant overhead as a packet may traverse PCIe bus twice, which not only consumes double PCIe bandwidth resource but also incurs a long delay. We choose to directly place out-of-order packets' data into application memory. This approach is simple and achieves optimal performance in most cases. However, to support applications that rely on the strict order of memory updates, e.g., key-value store using RDMA WRITE operations [14], MP-RDMA allows programmers to specify a *synchronise* flag on an operation, and MP-RDMA ensures that a synchronise operation updates the memory only after all previous operations are completed.

One straightforward approach is to delay a synchronise operation until the initiator receives acknowledgements or data

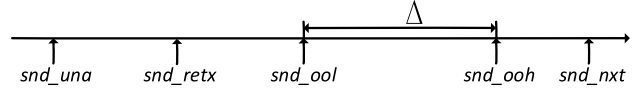


Fig. 5. MP-RDMA window structure at the sender.

(for READ verbs) of all previous operations. This may cause inferior performance as one additional RTT will be added to every synchronise operation. We mitigate this penalty by delaying synchronise operations only an interval that is slightly larger than the maximum delay difference among all paths. In this way, the synchronise operations should complete just after all its previous messages with high probability. With the out-of-order aware path selection mechanism (§III-C), this delay interval can be easily estimated as

$$\Delta t = \alpha \cdot \Delta / R_s = \alpha \cdot \Delta / \left(\frac{cwnd}{RTT} \right),$$

where Δ is the target out-of-order level, R_s is the sending rate of the RDMA connection and α is a scaling factor. We note that synchronise messages could still arrive before other earlier messages. In these rare cases, to ensure correctness, the receiver may drop the synchronise message and send a NACK, which allows the sender to retransmit the message later.

We note that the latest commodity RDMA NICs (e.g., Mellanox ConnectX-5 [36]) can also maintain original memory access order under out-of-order RDMA operations (called OOO mode). Nevertheless, they do not target for multi-path transport scenarios and their designs are not publicly available.

E. Other Design Details and Discussions

Loss Recovery: For single-path RDMA, packet loss is detected by the gap in PSNs. But in MP-RDMA, out-of-order packets are common and most of them are not related to packet losses. MP-RDMA combines loss detection with the out-of-order aware path selection algorithm. In normal situations, the algorithm controls OOD to be around Δ . However, if a packet gets lost, OOD will continuously increase until it is larger than the size of the tracking bitmap. Then, a NACK will be generated by the receiver to notify the PSN of the lost packet. Upon a NACK, MP-RDMA enters recovery mode. Specifically, we store the current snd_nxt value into a variable called *recovery* and set snd_retx to the NACKed PSN (Fig. 5). In the recovery mode, an incoming ACK clocks out a retransmission packet indicated by snd_retx , instead of a new packet. If snd_una moves beyond *recovery*, the loss recovery mode ends.

There is one subtle issue here. Since MP-RDMA enters recovery mode only upon bitmap overflow, if the application does not have that much data to send, RTO is triggered. To avoid this RTO, we adopt a scheme of FUSO [22] that early retransmits unacknowledged packets as new data if there is no new data to transmit and *awnd* allows. In rare case that the retransmissions are also lost, RTO will eventually fire and the sender will start to retransmit all unacknowledged packets.

Burst Control: Sometimes for a one returned ACK, the sender may have a burst of packets (≥ 2) to send, e.g., after exiting recovery mode. If all those packets are sent to the ACK's VP, the congestion may deteriorate. MP-RDMA forces that one ACK can clock out at most two data packets. The rest packets will gradually be clocked out by successive ACKs.

If no subsequent ACKs return, these packets will be clocked out by a *burst_timer* to random VPs. The timer length is set to wait for outstanding packets to be drained from the network, *e.g.* 1/2 RTT.

Path Window Reduction: If there is no new data to transfer, MP-RDMA gracefully shrinks *cwnd* and reduce the sending rate accordingly following a principle called “*use it or lose it*”. Specifically, if the sender receives an ACK that should kick out a new packet but there is no new data available, *cwnd* is reduced by one. This mechanism ensures that all sending paths adjust their rates independently. If path window reduction mechanism is not used, the sending window opened up by an old ACK may result in data transmission on an already congested path, thus deteriorating the congestion.

Connection Restart: When applications start to transmit data after idle (*e.g.* 1 RTO), MP-RDMA will restart from IW and restore multi-path ACK clocking. This is similar to the restart after idle problem in TCP [37].

Interact With PFC: With our ECN-based end-to-end congestion control, PFC will seldom be triggered. If PFC pauses all transmission paths [2], [3], MP-RDMA will gradually stop sending since no data packet arrives at the receiver and no ACK returns. When PFC resumes, ACK clocking will be restarted. If only a subset of paths are paused by PFC, those paused paths will gradually be eliminated by the OOO-aware path selection due to their longer delay. We have confirmed above arguments through simulations. We omit the results here due to space limitation.

IV. FLUID MODEL ANALYSIS OF MP-RDMA CONGESTION CONTROL

We develop a fluid model for MP-RDMA congestion control. For clarity, we first establish a single-path model for MP-RDMA to show its ability to control the queue oscillation. Then a multi-path model is given to demonstrate its ability in balancing congestion among multiple paths. We assume all flows are synchronized, *i.e.* their window dynamics are in phase. This fluid model only focuses on the congestion control algorithm in MP-RDMA, and we assume that OOO path selection and synchronise mechanism are not triggered.

A. Single-Path Model

Consider N long-lived flows traversing a single-bottleneck link with capacity C . The following functions describe the dynamics of $W(t)$ (congestion window), $q(t)$ (queue size). We use $R(t)$ to denote the network RTT, $F(t)$ to denote the ratio of ECN marked packets in the current window of packets. d is the propagation delay. We further use $R^* = d + \text{average_queue_length}/C$ to denote the average RTT. MP-RDMA tries to strictly hold the queue length around a fixed value, thus R^* is fixed:

$$\frac{dW}{dt} = \frac{1 - F(t - R^*)}{R(t)} - \frac{W(t)}{2R(t)}F(t - R^*) \quad (1)$$

$$\frac{dq}{dt} = N \frac{W(t)}{R(t)} - C \quad (2)$$

$$R(t) = d + \frac{q(t)}{C} \quad (3)$$

Eq. (1) models the flow’s window dynamics, which consists of the increase and the decrease term. Eq. (2) models the queue evolution on the bottleneck link, where $N \frac{W(t)}{R(t)}$ is the input

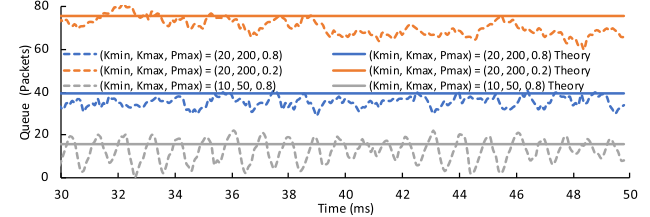


Fig. 6. Single-path fluid model simulation results.

rate and C is the service rate. Eq. (3) models the RTT which is sum of the propagation delay and the queuing delay.

The fix point of Eq. (1) is: $W = \frac{2(1-F)}{F}$. Eq. (2) gets that $q(t) = NW(t) - CR(t) + k$, where k is an arbitrary constant. Let $k = 0$ and combine Eq. (2) and (3), which gives:

$$q = \frac{NW}{2} - \frac{Cd}{2} = \frac{N(1-F)}{F} - \frac{Cd}{2} \quad (4)$$

MP-RDMA requires RED marking at the switch [34], which gives the following ECN marking function:

$$F = \begin{cases} 0 & \text{if } q \leq K_{\min} \\ P_{\max} \frac{q - K_{\min}}{K_{\max} - K_{\min}} & \text{if } K_{\min} < q \leq K_{\max} \\ 1 & \text{if } q > K_{\max} \end{cases} \quad (5)$$

Combining Equation (4) and (5) yields the fix point solution (q, W, F) .

We use NS3 [38] simulations to validate our analysis. 8 flows each with output rate 10Gbps, compete for a 10Gbps bottleneck link. RTT is set to 100μs. We test three RED settings, *i.e.*, $(K_{\min}, K_{\max}, P_{\max}) = (20, 200, 0.8)$, $(K_{\min}, K_{\max}, P_{\max}) = (20, 200, 0.2)$, and $(K_{\min}, K_{\max}, P_{\max}) = (10, 50, 0.8)$. Fig. 6 compares the simulation results with the theory value calculated according to our fluid model.

We can see that our model has well matched the actual queue length under various settings. Moreover, **MP-RDMA achieves a stable queue with very small oscillation**, with proper RED settings (*i.e.*, there is enough gap between K_{\min} and K_{\max}). We found that with smaller difference between K_{\min} and K_{\max} , the queue oscillation would be larger. This is because when the ECN marking curve is steep, the marking process is not that continuous. It is easy to see that if $K_{\min} = K_{\max}$ (which is the marking function used in DCTCP), as MP-RDMA doesn’t use any history ECN information, MP-RDMA can be modeled as a per-packet case of DCTCP with $g = 1$, which has large queue oscillation [39]. The accurate stability analysis requires complicated mathematical tools [39], which is beyond the scope of this paper.

We have also compared the queue oscillation of our MP-RDMA with DCTCP and TCP. For DCTCP, we use the recommended settings in the paper ($g = 1/16$ and $K = 40$). For TCP, we use two ECN marking schemes, *i.e.*, $K_{\min} = K_{\max} = 40$ as in DCTCP (denoted as TCP Instant-Mark) and standard RED with $(K_{\min}, K_{\max}, P_{\max}) = (20, 200, 0.8)$ as in MP-RDMA (denoted as TCP RED). Fig. 7 shows the results in the same simulation scenario before. Among all the schemes, MP-RDMA has the smallest queue oscillation. This is benefited from MP-RDMA’s per-packet *cwnd* adjustment behavior which is more like a continuous process than other schemes’ per-RTT *cwnd* adjustment.

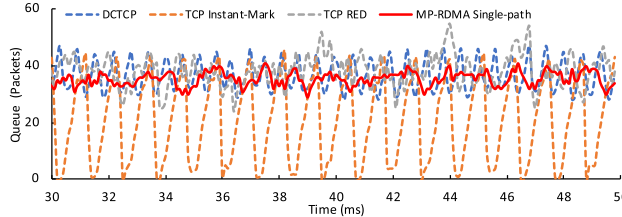


Fig. 7. Single-path queue oscillation compared with DCTCP and TCP.

B. Multi-Path Model

Now we develop the multi-path model. Consider an MP-RDMA flow k . Let VP_{ki} denote i th VP of flow k . We assume VP_{ki} has a virtual $cwnd$ denoted by w_{ki} , which controls the number of packets on VP_{ki} . And the total $cwnd_k$ is given as $cwnd_k = \sum_i w_{ki}$. We use ϵ to denote the fraction part of $cwnd_k$, i.e. $\epsilon = cwnd_k - \lfloor cwnd_k \rfloor$. We assume ϵ has a uniform distribution from 0 to 1 (denoted as $U[0, 1)$).⁶

An ECN ACK from VP_{ki} will reduce $cwnd_k$ by $1/2$ segment. There could be two situations: If $\epsilon \geq 1/2$, a new packet can still be clocked out on path VP_{ki} ; otherwise, after reduction, the new $cwnd_k$ will prevent a packet from sending to VP_{ki} . Since ϵ is subject to $U(0, 1)$, an ECN ACK reduces w_{ki} by one with probability 50%. On the other hand, a non-ECN ACK increases $cwnd_k$ by $1/cwnd_k$. If the growth of $cwnd_k$ happens to allow one additional packet, VP_{ki} would get two packets. As ϵ is subject to $U(0, 1)$, such chance would be equal for each incoming non-ECN ACK, i.e. $1/cwnd_k$. In other words, a non-ECN ACK increases w_{ki} by one with probability $1/cwnd_k$.

Based on the above analysis, we can establish the fluid model for our multi-path congestion control. Consider N flows, each flow distributes their traffic to M_v virtual paths, which are mapped onto M_p physical paths. We use $Path(kj)$ to denote the set of flow k 's virtual paths that are mapped onto physical path j . R_{ki} and F_{ki} denote the flow k 's RTT and ECN marking ratio on the i th VP, respectively. Similar to the single-path, we have the following multi-path fluid model:

$$(k = 1, 2, \dots, N; i = 1, 2, \dots, M_v; j = 1, 2, \dots, M_p)$$

$$\frac{dw_{ki}}{dt} = \frac{w_{ki}(t)}{cwnd_k(t) * R_{ki}(t)} [1 - F_{ki}(t - R_{ki}^*)] - \frac{w_{ki}(t)}{2R_{ki}(t)} F_{ki}(t - R_{ki}^*) \quad (6)$$

$$\frac{dq_j}{dt} = \frac{\sum_{k=1}^N \sum_{i \in Path(kj)} w_{ki}(t)}{R_j(t)} - C_j \quad (7)$$

$$R_j(t) = d_j + \frac{q_j(t)}{C_j} \quad (8)$$

Eq. (6) models the k th flow's window dynamics on its i th virtual path. Eq. (7) models the queue evolution on each physical path, where $\sum_{k=1}^N \sum_{i \in Path(kj)} w_{ki}(t)/R_j(t)$ is the input rate on the j th physical path and C_j is its service rate. Eq. (8) models the RTT on each physical path.

⁶We note that this assumption cannot be easily proven as the congestion window dynamics are very complicated, but our observation on both testbed and simulation experiments verified the assumption. Later we will show that based on this assumption, our experiments and theoretical analysis results match each other very well.

Eq. (6) yields the fix point solution:

$$F_{ki} = \frac{2}{cwnd_k + 2} \quad (9)$$

As F_{ki} only depends on the total $cwnd_k$, this indicates that each flow's marking ratio on each VP will be the same. In other words, **MP-RDMA can balance a flow's ECN marking ratio among all its virtual paths regardless of their physical mapping and their RTTs, capacities and RED marking curves**. Furthermore, since the VPs which are mapped to the same physical path experience the same ECN RED marking function, their marking ratio should be the same which equals the physical path's marking ratio. As such, the marking ratio on all the physical paths that a flow used should be the same. In datacenters where all equal-cost paths have same capacities and RED marking curves, **MP-RDMA can balance the load among all the parallel paths**.

Since all flows use the same M_p physical paths, it is easy to derive that all flows' ECN marking ratio on all VPs are the same. As such, along with Eq. (9), we get

$$cwnd_{k_1} = cwnd_{k_2}, \text{ for any } k_1, k_2 \in 1, \dots, N \quad (10)$$

In fact, above equation is valid for any two flows k_1 and k_2 if there exists a VP i_1 of flow k_1 and a VP i_2 of flow k_2 that i_1 and i_2 are mapped to the same physical path. This indicates that **all MP-RDMA flows that compete the same path will converge to the same stable throughput**.

We now try to derive the exact fix point solution of $(q, F, cwnd)$ on each path in terms of each path's RTT, capacity and RED parameters. Similar as before, from Eq. (7) and (8), the queue can be calculated as:

$$q_j = \frac{\sum_{k=1}^N \sum_{i \in Path(kj)} w_{ki}(t)}{2} - \frac{C_j d_j}{2} \quad (11)$$

Combining Eq. (9), (11) and the path's RED marking function in Eq. (5), we get

$$\frac{2}{cwnd_k + 2} = P_{max_j} \frac{\frac{\sum_{k=1}^N \sum_{i \in Path(kj)} w_{ki}(t)}{2} - \frac{C_j d_j}{2} - K_{min_j}}{K_{max_j} - K_{min_j}} \quad (12)$$

Since $\sum_{k=1}^N cwnd_k = \sum_{k=1}^N \sum_{j=1}^{M_p} \sum_{i \in Path(kj)} w_{ki}(t)$, combining with Eq. (10), we can have the fix point solution of $(q, F, cwnd)$.

We use simulations to validate our conclusion. 10 MP-RDMA connections are established. Each sends at 40Gbps among 8 VPs. The virtual paths are mapped randomly onto 4 physical paths. The network base RTT of each path is set to 16μs. We test three different network settings with $C_{1,2,3,4} = (20G, 40G, 60G, 80G)$ $P_{max_{1,2,3,4}} = (0.2, 0.4, 0.6, 0.8)$, $C_{1,2,3,4} = (20G, 40G, 60G, 80G)$ $P_{max_{1,2,3,4}} = (0.8, 0.8, 0.8, 0.8)$ and $C_{1,2,3,4} = (80G, 80G, 80G, 80G)$ $P_{max_{1,2,3,4}} = (0.8, 0.8, 0.8, 0.8)$, respectively. Also, we test two VP mapping conditions with each flow has 8 VPs and 2 VPs respectively. Fig. 8 and 9 show the ECN marking ratio and the queue length of the 4 physical paths and the $cwnd$ of each flow under 8 VP and 2 VP conditions, respectively. Results show that the ECN marking ratio, queue length and $cwnd$ all match well to the theory values calculated from our fluid model.

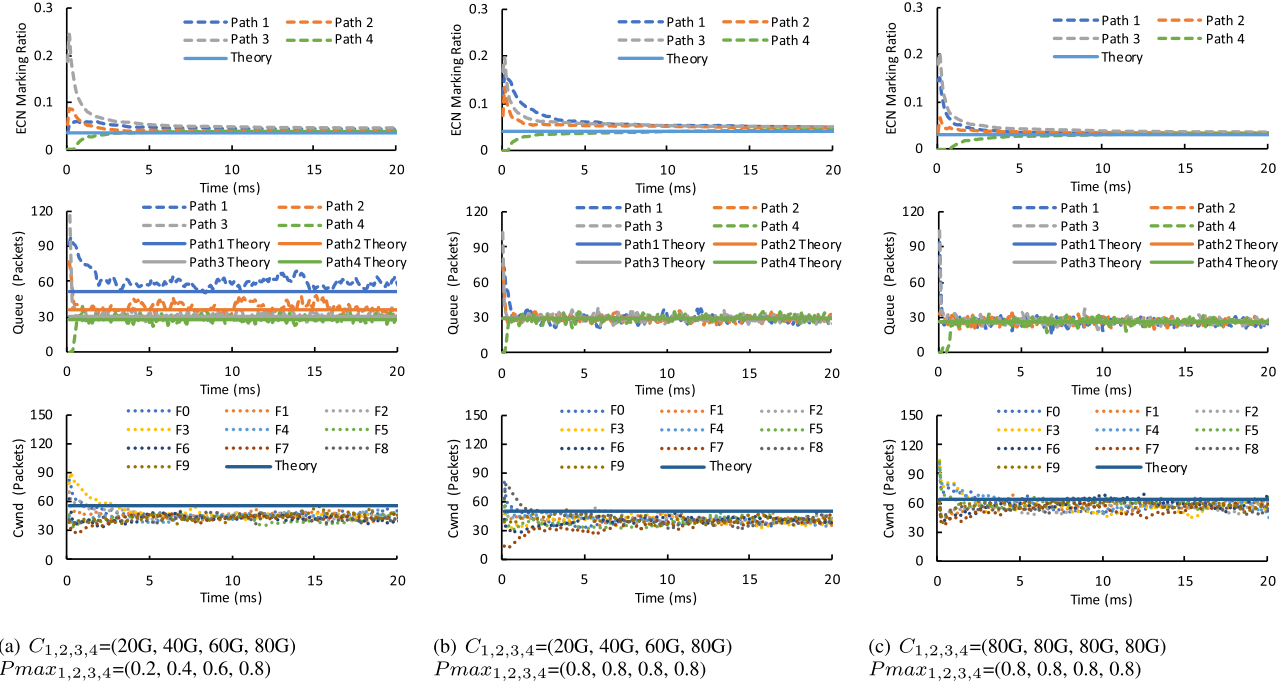


Fig. 8. Multi-path fluid model simulation results. Each flow uses 8 virtual paths.

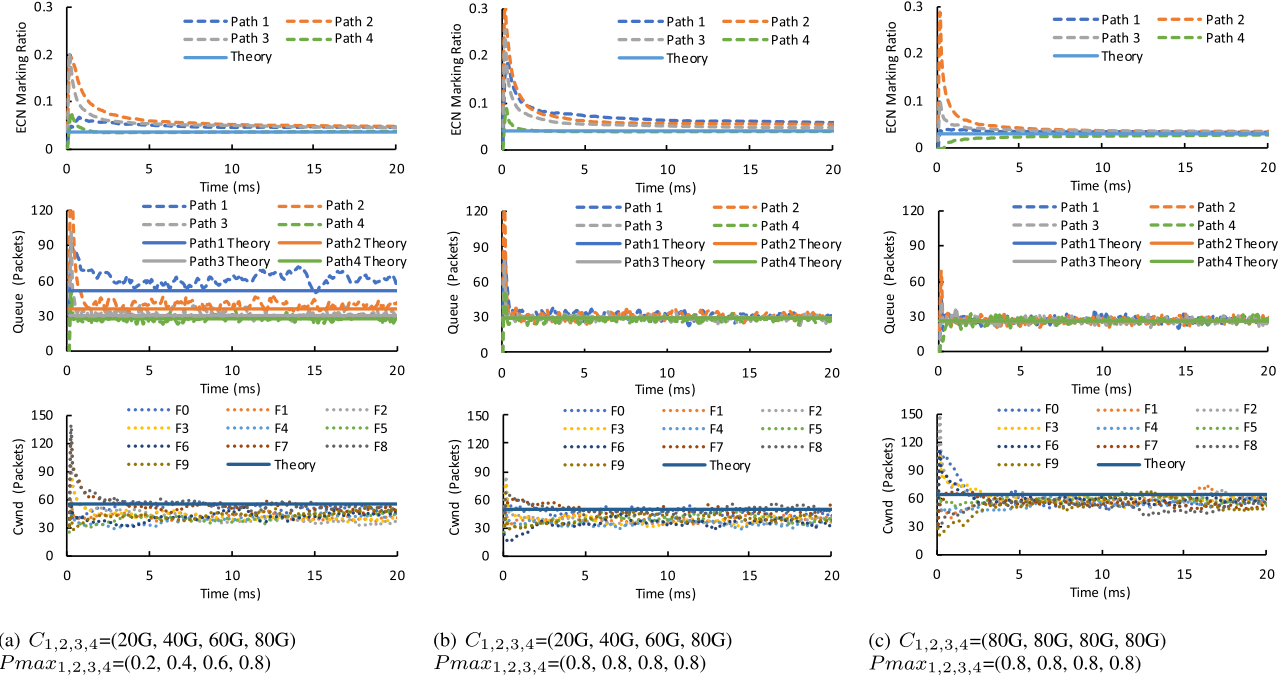


Fig. 9. Multi-path fluid model simulation results. Each flow uses 2 virtual paths.

Moreover, the results have verified our conclusion that all paths will converge to the same ECN marking ratio, and all flows will converge to the same throughput (*i.e.*, same *cwnd*).

V. IMPLEMENTATION

A. FPGA-Based Prototype

We have implemented an MP-RDMA prototype using Altera Stratix V D5 FPGA board [40] with a PCIe Gen3 x8 interface and two 40G Ethernet ports. Fig.10 shows

the overview of the prototype architecture. There are two major components: 1) MP-RDMA transport logic, and 2) MP-RDMA library. The entire transport logic is implemented on FPGA with ClickNP framework [41]. We have developed 14 ClickNP elements with ~2K lines of OpenCL code. Applications call MP-RDMA library to issue operations to the transport. FPGA directly DMAs packet data from/to the application buffer via PCIe.

Table I summarizes all extra states incurred per connection by MP-RDMA for multi-path transport compared to

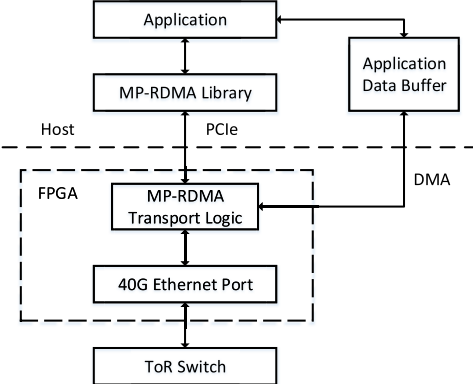


Fig. 10. System architecture.

TABLE I
MP-RDMA STATES

Functionality	Variable	Size (B)
Congestion control	<i>cwnd</i>	4
	<i>inflate</i>	4
	<i>snd_una</i>	3
	<i>snd_nxt</i>	3
	<i>rcv_nxt</i>	3
OOO-aware path selection	<i>snd_ooh</i>	3
	<i>L</i>	1
Loss recovery	<i>snd_retx</i>	3
	<i>recovery</i>	3
Path probing	<i>MaxPathID</i>	2
	<i>p</i>	1
Tracking OOO packets	<i>bitmap</i> data	16
	<i>bitmap</i> head	1
Burst Control	<i>burst_timer</i>	3
Connection restart	<i>restart_timer</i>	3
Synchronise message	α	1
RTT measurement	<i>srtt, rtvar, rtt_seq</i>	12
Total	N/A	66

existing RoCE v2. Collectively, MP-RDMA adds additional 66 bytes. This extra memory footprint is comparable to other single-path congestion control proposals to enhance RoCE v2. For example, DCQCN [2] adds ~60 bytes for its ECN based congestion control.

B. Validation

We now evaluate the basic performance of the FPGA-based prototype. We measure the processing rate and latency for sending and receiving under different message sizes. Specifically, the sending/receiving latency refers to the time interval between receiving one ACK/data packet and generating a new data/ACK packet.

To measure the processing rate for sending logic, we use one MP-RDMA sender to send traffic to two MP-RDMA receivers, creating a sender bottleneck, vice versa for measuring the receiving logic. As shown in Fig.11, our implementation achieves line rate across all message sizes for receiving. For sending, when message size is smaller than 512 bytes, the sender cannot reach the line rate. This is because sender logic is not fully pipelined due to memory dependencies. However, our sending logic processing rate is still 10.4%~11.5% better than commodity Mellanox RDMA NIC (ConnectX-3 Pro) [42], [43]. When message size is larger, *i.e.* >512B, the sender logic can sustain the line-rate of 40Gbps. The prototype also achieves low latency. Specifically, the sending and receiving latency is only 0.54 μ s and 0.81 μ s for 64B messages respectively.

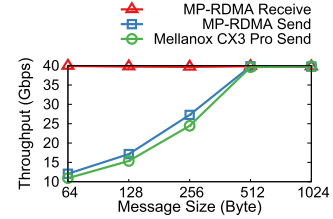


Fig. 11. Prototype ability.

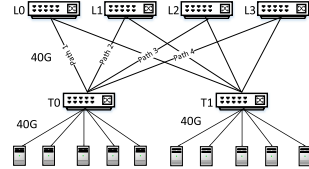


Fig. 12. Testbed topology.

VI. EVALUATION

In this section, we first evaluate MP-RDMA's overall performance. Then, we evaluate properties of MP-RDMA algorithm using a series of targeted experiments.

Testbed Setup: Our testbed consists of 10 servers located under two ToR switches as shown in Fig.12. Each server is a Dell PowerEdge R730 with two 16-core Intel Xeon E5-2698 2.3GHz CPUs and 256GB RAM. Every server has one Mellanox ConnectX-3 Pro 40G NIC as well as an FPGA board that implements MP-RDMA. There are four switches connecting the two ToR switches forming four equal-cost cross-ToR paths. All the switches are Arista DCS-7060CX-32S-F with Trident chip platform. The base cross-ToR RTT is $12\mu s$ (measured using RDMA ping). This means the bandwidth delay product for a cross-ToR network path is around 60KB. We enable PFC and configure RED with $(P_{max}, K_{min}, K_{max}) = (1.0, 20KB, 20KB)$ as it provides good performance on our testbed. The initial window is set to be one BDP. We set $\Delta = 32$ and the size of the bitmap $L = 64$.

A. Benefits of MP-RDMA

1) Robust to Path Failure:

a) Lossy paths: We show that MP-RDMA can greatly improve RDMA throughput in a lossy network [11].

Setup: We start one RDMA connection from T0 to T1, continuously sending data at full speed. Then, we manually generate random drop on Path 1, 2 and 3. We leverage the switch built-in iCAP (ingress Content-Aware Processor) [44] functionality to drop packets with certain IP ID (*e.g.*, $ID \bmod 100 == 0$). We compare the goodput between MP-RDMA and single-path RDMA (DCQCN). Each result is the average of 100 runs.

Results: Fig.13(a) illustrates that MP-RDMA always achieves near to optimal goodput (\sim 38Gbps excluding header overhead) because it always avoids using lossy path. Specifically, the credits on lossy paths are gradually reduced and MP-RDMA moves its load to Path 4 (good path). However, DCQCN has 75% probability to transmit data on lossy paths. When this happens, DCQCN's throughput drops dramatically due to its go-back-N loss recovery mechanism. Specifically, the throughput of the flow traversing lossy path drops to \sim 10Gbps when the loss rate is 0.5%, and drops to near zero when loss rate exceeds 1%. This conforms with the

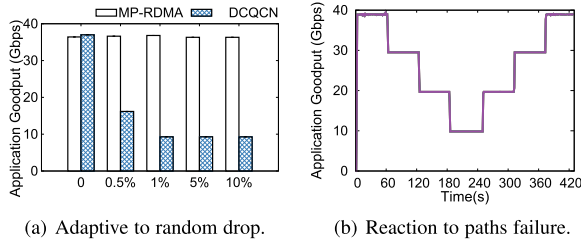


Fig. 13. MP-RDMA robustness.

results in [2], [45]. As a result, DCQCN can achieve only ~ 17.5 Gbps average goodput when loss rate is 0.5%. When the loss rate exceeds 0.5%, DCQCN achieves only $\sim 25\%$ average goodput compared with MP-RDMA. Improving the loss recovery mechanism (*e.g.*, [45]) is a promising direction to further improve the performance of MP-RDMA and DCQCN, but it is not the focus of this paper.

b) Quick reaction to link up and down:: We show that MP-RDMA can quickly react to path failure and restore the throughput when failed paths come back.

Setup: We start one MP-RDMA connection from T0 to T1 and configure each path to be 10Gbps. At time 60s, 120s, and 180s, P1, P2, and P3 are disconnected one by one. At time 250s, 310s, and 370s, these paths are restored to healthy status one by one.

Results: Fig.13(b) shows that, upon each path failure, MP-RDMA quickly throttles the traffic on that path, meanwhile fully utilizes other healthy paths. This is because there are no ACKs returning from the failed paths which leads to zero traffic on those paths. While the ACK clocking for healthy paths is not impacted, those paths are fully utilized and are used to recover the lost packets on failed paths. When paths are restored, MP-RDMA can quickly fully utilize the newly recovered path. Specifically, for each restored path, it takes only less than 1s for this path to be fully utilized again. This is benefited from the path probing mechanism of MP-RDMA, which periodically explores new VPs and restores the ACK-clocking on those paths.

2) Improved Overall Performance: Now, we show that with multi-path enabled, the overall performance can be largely improved by MP-RDMA.

a) Small-scale testbed: Now we evaluate the throughput performance on our testbed.

Setup: We generate a permutation traffic [5], [25], where 5 servers in T0 setup MP-RDMA connects to 5 different servers in T1 respectively. Permutation traffic is a common traffic pattern in datacenters [2], [3] and in the following, we use this pattern to study the though-put, latency and out-of-order behavior of MP-RDMA. We compare the overall goodput (average of 10 runs) of all these 5 connections of MP-RDMA with DCQCN.

Results: The results show that MP-RDMA can well utilize the link bandwidth, achieving in total 150.68Gbps goodput (near optimal excluding header overhead). Due to the coarse-grained per-connection ECMP-based load balance, DCQCN only achieves in total 102.46Gbps. MP-RDMA gains 47.05% higher application goodput than DCQCN. Fig.14(a) shows the goodput of each RDMA connection (denoted by its originated server ID) in one typical run. The 5 flows in MP-RDMA fairly share all the network bandwidth and each achieves ~ 30 Gbps. However, in DCQCN, only 3 out of 4 paths are used for

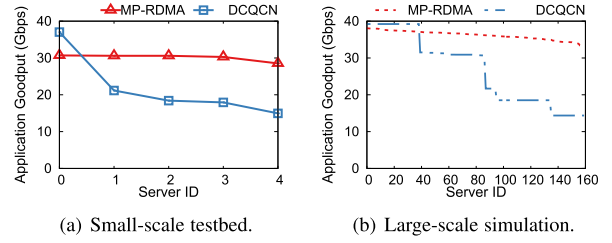


Fig. 14. Overall throughput compared with DCQCN.

transmission while the other one path is idle, which leads to much lower (<20Gbps) and imbalanced throughput.

b) Large-scale simulation on throughput: Now we evaluate throughput performance at scale with NS3 [38].

Setup: We build a leaf-spine topology with 4 spine switches, 32 leaf switches and 320 servers (10 under each leaf). The server access link is 40Gbps and the link between leaf and spine is 100Gbps, which forms a full-bisection network. The base RTT is 16us. For the single-path RDMA (DCQCN), we use the simulation code and parameter settings provided by the authors. We use the same permutation traffic [5], [25] as before. Half of the servers act as senders and each sends RDMA traffic to one of the other half servers across different leaf switches. In total there are 160 RDMA connections. For MP-RDMA, the ECN threshold is set to be 60KB.

Results: Fig.14(b) shows the goodput of each RDMA connection. MP-RDMA achieves much better overall performance than DCQCN with ECMP. To be specific, the average throughput of all servers of MP-RDMA is 34.78% better than DCQCN. Moreover, the performance across multiple servers is more even in MP-RDMA, where the lowest connection throughput can still achieve 32.95Gbps. However, in DCQCN, many unlucky flows are congested into a single path, leading to a very low throughput (*e.g.*, <15Gbps) for them.

c) Large-scale simulation on FCT: *Setup:* We use the same leaf-spine topology and generate flow size according to a web search workload [46]. The source and destination of each flow are randomly picked from all the servers. We further assume that flows arrive according to a Poisson process and vary the inter-arrival time of flows to form different levels of load.

Results: In this experiment, at start up, each connection uses 54 virtual paths. As time goes by, a long flow will result in using about 60~70 virtual paths. Fig. 15 shows the normalized FCT performance. For average FCT, MP-RDMA is 6.0%~17.7% better than DCQCN. For large flows (>10MB), throughput is the dominate factor. As MP-RDMA avoids hash collision, they achieve 16.7%~77.7% shorter FCT than DCQCN. We omit the figure due to space limitation. For small flows (<100KB), MP-RDMA also achieves a little bit better FCT (3.6%~13.3% shorter) than DCQCN [Fig. 14(b)]. This advantage is from finer grained load balance and accurate queue length control of congestion control (§IV) in MP-RDMA.

B. MP-RDMA Deep-Dive

1) OOO-Aware Path Selection: Now, we show MP-RDMA’s OOO-aware path selection algorithm can well control the OOO degree, and achieve good application throughput.

Setup: We use the same traffic as in §VI-A.2, and measure the OOO degrees in three different scenarios:

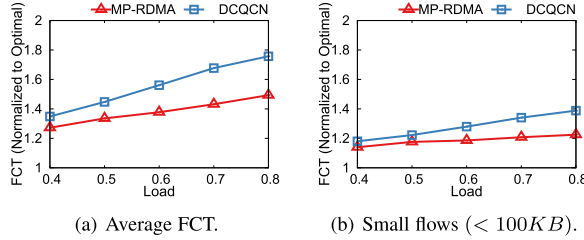


Fig. 15. FCT performance compared with DCQCN.

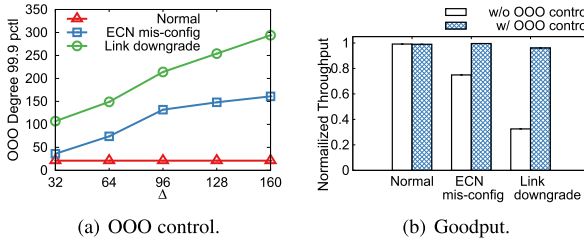


Fig. 16. Out-of-order control algorithm performance.

1) *Normal*, in which all paths RED marking parameters are configured as $(P_{max}, K_{min}, K_{max}) = (1.0, 20KB, 20KB)$; 2) *ECN mis-configure*, in which the RED of path 4 is mis-configured as $(P_{max}, K_{min}, K_{max}) = (1.0, 240KB, 240KB)$; 3) *link-degradation*, in which path 4 degrades from 40Gbps to 1Gbps due to failure caused auto-negotiation.

Results: First we set bitmap length L to infinite to cover the maximum OOD. Then, we evaluate how MP-RDMA can control the OOD to different extent with different Δ . Fig. 16(a) shows the 99.9th percentile of OOD using different Δ under various scenarios. OOO-aware path selection can well control the OOD. Specifically, compared to MP-RDMA without OOO control,⁷ $\Delta = 32$ can effectively reduce the OOD 99.9th by $\sim 5\times$ and $\sim 50\times$ under *ECN mis-configuration* and *link-degradation* respectively. A proper Δ can control the OOD to a small range, which means that we can use a very small L in practice under various network conditions.

Next, we consider a bitmap with $L = 64$. We set $\Delta = 32$ correspondingly. Fig. 16(b) shows the throughput normalized to the ideal case when all connections fairly share the full bandwidth. With OOO control, in *ECN mis-configure* case, MP-RDMA achieves optimal throughput. Even in more extreme *link-degradation* case, the overall application throughput is only 3.94% less than the optimal. However, if MP-RDMA uses the same $L = 64$ bitmap but without OOO control, its throughput significantly degrades by 25.1% and 67.5% under these two cases respectively, due to severe OOO.

2) *Congestion-Aware Path Selection*: Now, we show MP-RDMA's ability to do congestion-aware traffic distribution.

Setup: We configure each path to 10G and start one MP-RDMA long connection sending unlimited data at the maximum rate. Normally, the traffic is evenly balanced among the four parallel paths. Then after ~ 30 s, we start another special MP-RDMA flow which is manually forced to use only Path 4 (denoted as SP-RDMA). The SP-RDMA flow will cause a sudden congestion on Path 4. We evaluate how MP-RDMA perceives the congestion and moves the load away from Path 4.

⁷Without OOO control, the 99.9th OOD is 179 and 5324 for the two abnormal scenarios, respectively.

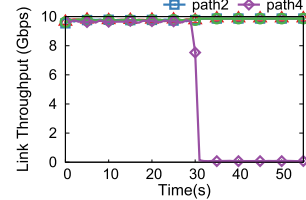


Fig. 17. Path selection.

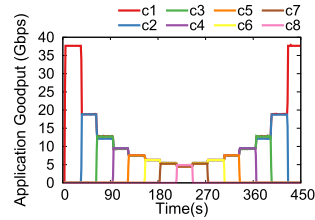


Fig. 18. MP-RDMA fairness.

Results: Fig. 17 shows the throughput of the MP-RDMA flows on each of the four paths. Before the SP-RDMA flow joins, each path has a throughput stable at ~ 10 Gbps. After the SP-RDMA joins on Path 4, the throughput of the MP-RDMA flows on Path 4 quickly falls to near zero. Meanwhile, the throughput on other 3 paths all remains at around 10Gbps. This indicates that MP-RDMA can quickly perceive the congestion on Path 4, and moves the load away from this path. Also, since the congestion conditions on other paths remain unchanged, MP-RDMA does not adjust the load on them. Here we don't focus on the fairness between SP-RDMA and MP-RDMA connections.

3) *Fairness of MP-RDMA* : *Setup*: In this experiment, two physical servers under one ToR establish multiple MP-RDMA connections to another server under the same ToR creating a single bottleneck. 8 MP-RDMA connections are started one by one with an interval of 30s, and then leaves the network one after another with the same time interval. We measure the application goodput of each connection.

Results: Fig. 18 shows that all flows evenly share the network, and get the fair share quickly. Specifically, each connection's throughput quickly converges to $\sim \frac{40}{n}$ Gbps, when n varies from 1 to 8 and then 8 to 1. The Jain fairness index [47] is within 0.996 - 0.999 (1 is optimal) under various number of concurrent flows.

4) *Incast*: Next we evaluate MP-RDMA's congestion control under more stressed scenario, *i.e.*, incast.

Setup: The traffic pattern mimics a disk recovery service [2] where failed disks are repaired by fetching backups from several other servers. Specifically, a receiver host initiates one connection with each of the N randomly selected sender host, simultaneously requesting 1Gb data from each sender. Following the convention in DCQCN [2], we vary the incast degree from 1 to 9. The experiment is repeated five times. We evaluate the overall application goodput at the receiver end.

Results: Fig. 19 shows that MP-RDMA achieves similar near-optimal incast performance as DCQCN. To be specific, when incast degree increases from 1 to 9, the total goodput of the 5 connections remains stable, at around 37.65Gbps. Note that MP-RDMA achieves a little ($\sim 3\%$) higher goodput than DCQCN. We cannot ascertain the exact root cause of this, but we believe this may be an implementation issue with the Mellanox NIC instead of an algorithm issue with DCQCN.

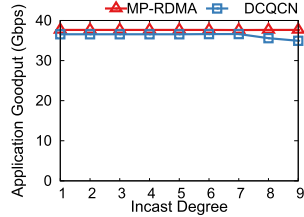


Fig. 19. Incast performance.

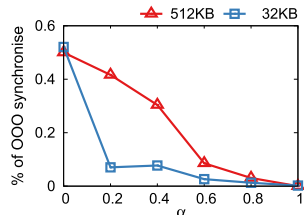
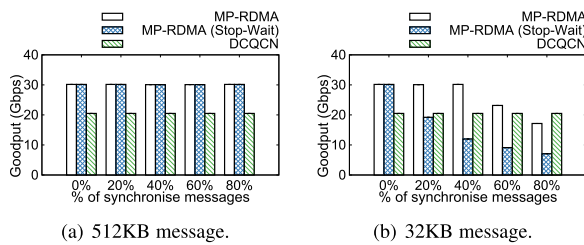
Fig. 20. α impact.

Fig. 21. Synchronise mechanism performance.

5) *Synchronise Mechanism Performance*: In this section, we evaluate the impact of *synchronise* mechanism on application performance.

Setup: The same permutation traffic in §VI-A.2 is used to emulate a typical network congestion. *Synchronise* messages will be delayed for a while and then send out. This results in burst traffic and causes large delay fluctuations. We stress test the mechanism under the case when the load is as high as 0.8. We first study the setting of parameter α by measuring the amount of out-of-order *synchronise* messages under different α . Then α is set to a value that ensures all the *synchronise* messages are in order. The average goodput for the 5 connections under various ratio of *synchronise* messages are measured. Two different message sizes are evaluated, *i.e.*, 512KB (RDMA-based RPC application [12]) and 32KB (a more challenging smaller size). The results are compared with DCQCN, which achieves only \sim 20Gbps in average (due to ECMP hash collision). We also evaluate MP-RDMA (Stop-Wait), in which a *synchronise* message is sent only when all previous messages are completed.

Results: As shown in Fig 20, larger α leads to less OOO *synchronise* messages. Under the same α , OOO is severer for larger message size due to the more congested network. When α is 1.0, no OOO occurs in our tests. As such, we set α to 1.0 for the following experiment.

Fig. 21 shows the result for *synchronise* mechanism impact on throughput. When message size is large (*e.g.*, 512KB), both MP-RDMA and MP-RDMA (Stop-Wait) can achieve \sim 30Gbps goodput, which is \sim 48% higher than single-path DCQCN across all *synchronise* ratios. This is because the Δt for sending *synchronise* messages is \sim 0.5 RTT for MP-RDMA and \sim 1 RTT for MP-RDMA (Stop-Wait). Both are rather

small compared with the transmission delay for a 512KB message. Thus the impact of Δt is amortized. When message size is smaller (*i.e.*, 32KB), Δt is larger compared with the message transmission delay. Thus the goodput drops as the *synchronise* message ratio grows. However, with our optimistic transmission algorithm (§III-D), MP-RDMA still achieves good performance. Specifically, MP-RDMA gets 13%~49% higher throughput than DCQCN under 0~60% *synchronise* ratio. When the *synchronise* ratio grows to 80%, MP-RDMA performs 16.28% worse. Note that this is already the worst case performance for MP-RDMA because the traffic load is at its peak, *i.e.* 100%. More results (omitted due to space limitation) show that, when the load is lighter, MP-RDMA performs very close to DCQCN under high *synchronise* ratio. On the contrary, the naive MP-RDMA (Stop-Wait) only achieves less than 50% throughput of MP-RDMA.

VII. RELATED WORK

Various multi-path transmission mechanisms propose to utilize parallel network paths in datacenters [5]–[7], [25], [28]–[33], [48]. Most of them consider only TCP, and cannot be directly used for RDMA.

Load-Balance Routing

Previous approaches such as [6], [7], [25], [28]–[33], [48] propose to balance traffic over a set of paths at the routing layer. In order to handle out-of-order packets, some of them, *e.g.*, [25], [32], utilize a dedicated reordering buffer under the transport layer. However, these schemes are hard to implement in NIC hardware. Other work, *e.g.*, [6], [33], try to proactively avoid out-of-order delivery. Most of them utilize *flowlets*. If the inactive gap between flowlets is long enough, flowlets can be distributed to different paths without causing out-of-order. However, for RDMA which is implemented in hardware and usually smoothed with a rate-shaper, it is quite hard to find flowlets. To validate this, we study the flowlet characteristics of RDMA and compare it with TCP on our testbed. We measure the size of flowlets with various inactive intervals. For each experiment, we run 8 RDMA/TCP flows with size 2GB. Fig. 22 shows that it is really difficult to observe flowlets in RDMA traffic. When the inactive interval is larger than $2\mu s$, the flowlet size is strictly 2GB. In contrast, TCP does have flowlets. When we set the inactive gap to $100\mu s$, we observe many flowlets with size \sim 60KB. We conclude that flowlet-based load balancing schemes may not work well for RDMA traffic. A recent work [49] reports that flowlet can be used to do load balance for DCQCN traffic. This might be true for applications with an on-off traffic pattern, but not for applications that are throughput intensive. Moreover, as flowlets cannot guarantee out-of-order free, it's not clear how out-of-order RDMA packets would impact the performance in [49].

Multi-Path Transport

MPTCP modifies TCP to enable multi-path transmission [5], [50], [51]. The core idea is to split the original transport into several sub-flows and distribute packets among these sub-flows according to their congestion states. Thereby MPTCP adds additional states proportional to the number of sub-flows and explores a large re-ordering buffer at the transport layer to handle out-of-order packets. As aforementioned,

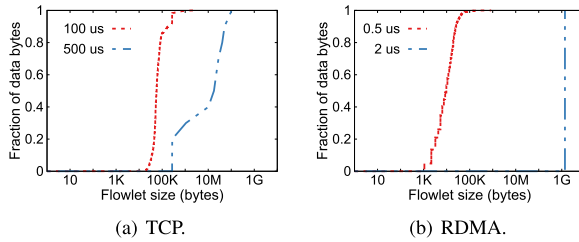


Fig. 22. Flowlet characteristics in TCP and RDMA.

this design adds considerable memory overhead and is difficult to implement in hardware.

Generally, the multi-path ACK-clocking of MP-RDMA resembles the PSLB algorithm [52] in the sense that both schemes adjust their load on multiple paths in a per-ACK fashion. However, MP-RDMA independently adjusts the load on each path while PSLB dynamically moves the load of slow paths to fast paths.

Recently Mellanox proposed a multi-path support for RDMA [53]. However, it is just a fail-over solution using two existing single-path RoCE connections (hot standby). The goal and the techniques of the Mellanox multi-path RDMA are completely different from MP-RDMA, which is a new multi-path RDMA transport.

VIII. DISCUSSION

A. Compare With Other Load-Balancing Routing and Multi-Path Transport

We use a simple simulation to compare the performance of MP-RDMA with CONGA [6], DRILL [48] and MPTCP [5], which are representative solutions of load-balancing routing (CONGA and DRILL) and multi-path transport (MPTCP) for datacenters, respectively. Note that we only target a quick and simple comparison of how well they utilize the multiple paths capacity in RDMA environment, rather than a comprehensive evaluation since neither CONGA, DRILL nor MPTCP are designed for RDMA and there are no existing works that discuss how to adapt them into RDMA environments.

We simulate a host that transmits a single RDMA flow with unlimited data to another host through a network with two parallel paths. Each path's capacity is 5Gbps and each host is connected to the network with a 10Gbps access link. The base RTT is 10us. We implement CONGA and DRILL on top of the RDMA NS3 simulation code [54] with DCQCN congestion control enabled. Note that although MPTCP consumes two much hardware resources which is not suitable for RDMA NIC implementation, here we ignore this practical limitation in the simulation so we can compare MPTCP with our MP-RDMA.

Fig. 23 shows the flow goodput and the transmission throughput measured on each path. Results show that MP-RDMA can fully utilize the two parallel paths and achieves about 10Gbps flow goodput, performing the same as MPTCP which uses multiple sub-flows to maintain per-path states.

CONGA cannot well utilize these two parallel paths. We evaluate various settings for the time length to divide flowlets in CONGA (called flowlet gap), i.e., 700us, 500us, 300us, 100us. Results show that when the flowlet gap is large (700us and 500us), an RDMA flow with DCQCN congestion control can only be divided into large flowlets. Hence it can only utilize one path for each period of time, and the flow

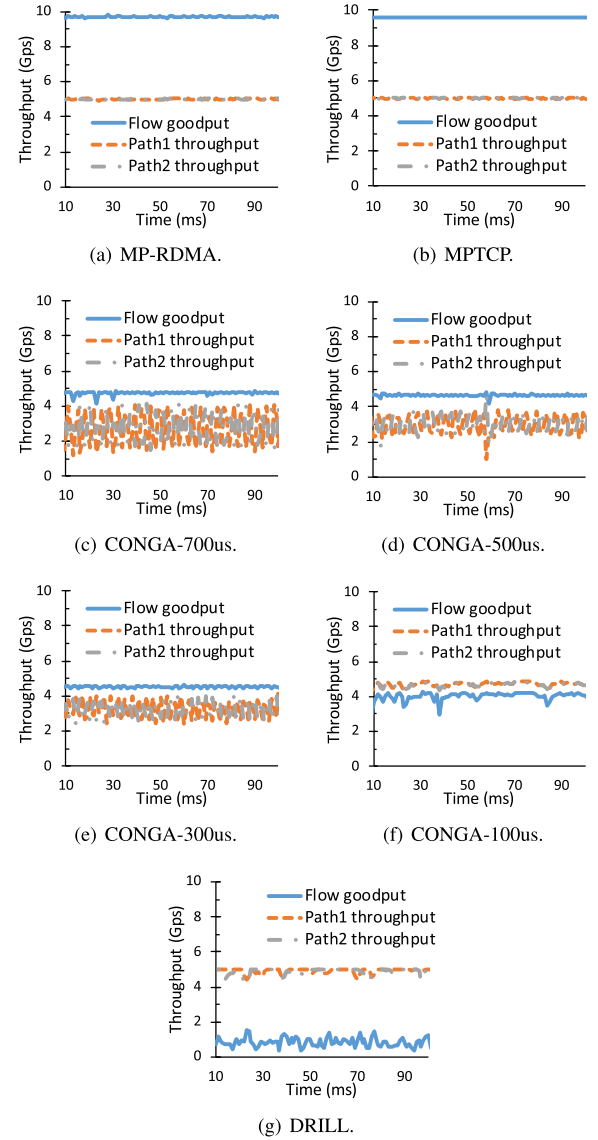


Fig. 23. Comparing MP-RDMA with MPTCP and CONGA.

goodput can only achieve about 5Gbps. However, when we decrease the flowlet gap, although flow packets now can be distributed on the two paths simultaneously, the small flowlet switching gap causes out-of-order arrival and the flow goodput even becomes lower because current RDMA transport is very sensitive to out-of-order and packet loss [2]. For example, when the flowlet gap is 100us, the transmission throughput on each path achieves about 5Gbps, but the overall flow goodput downgrades to about 4Gbps, because there are a lot out-of-order arrivals and many retransmissions on each path.

DRILL aggressively spreads packets to multiple output ports (randomly choose one of the shortest queues) at each switch, so it incurs significant packet out-of-order arrival at the receiver. Since existing RDMA NIC regards out-of-order arrival as packet loss and triggers go-back-N loss recovery, the overall throughput is degraded to only about 1Gbps (Fig. 23(g)), and there are many retransmitted packets on each path.

B. MP-RDMA Fairness Under Different MTUs

In order to evaluate MP-RDMA's fairness under different MTUs, we incur two long flows with different MTUs into

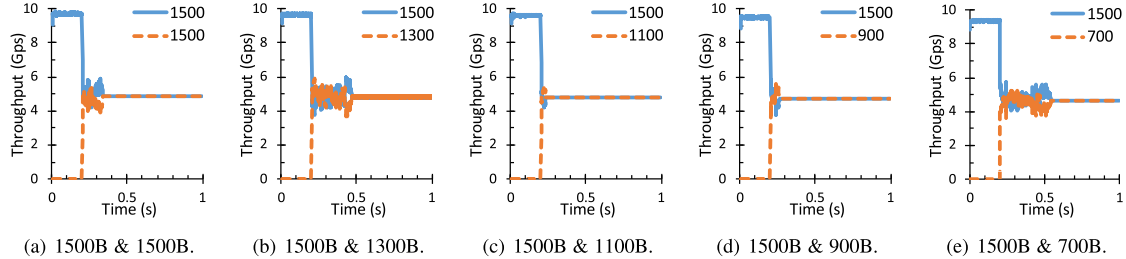


Fig. 24. Fairness between two flows with different MTUs.

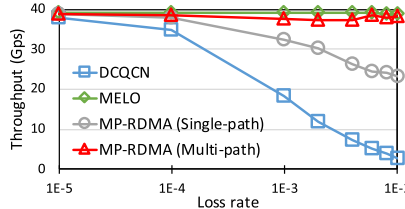


Fig. 25. Compare with advanced RDMA loss recovery schemes.

the network. The second flow joins after the first flow has run for 0.2 seconds. The other simulation settings are the same as in §VIII-A.

Fig. 24 shows the throughput of each flow as time grows. We can see that MP-RDMA can achieve good fairness among flows with various MTUs. The reason is that MP-RDMA flows will compete with the shared path according to the number of bytes, rather than the number of packets. Let us consider a simple example to analyze the flow speed changing trend under the steady state. We assume that a flow with 1500B MTU is competing with a flow with 750B MTU on the same link and both reach 50% of the link speed (which reaches the ideal fairness). The two flows will encounter the same ECN marking ratio, as they are in the same switch queue and the queue uses a certain marking curve according to the queue length (in bytes). Since the second flow has twice packets in the queue as the first flow (so their data speeds are equal because their MTUs are different), the second flow will get twice ECN marked ACKs back. As such, the second flow will decrease its *cwnd* twice as the first flow in terms of packets, which makes the *cwnd* decreasing amount equal in terms of bytes for the two flows. As such, their sending rate will keep the same and the fairness has been kept.

C. Compare With Other RDMA Loss Recovery Scheme

There are other recent works trying to improve RDMA's loss recovery [45], [55]. We compare MP-RDMA with an advanced RDMA loss recovery scheme, MELO [45], which enables SACK loss recovery for RDMA. Specifically, we use NS3 to simulate a network with two 40Gbps parallel paths, with one path having a random loss rate (from 0.001% to 1%). We inject a long flow into the network to see how different methods perform under such lossy condition. The other simulation settings are the same as before. We evaluate MP-RDMA under two scenarios. First, we force all VPs in MP-RDMA only going through the lossy path (denoted as MP-RDMA (Single-path)), to evaluate the loss recovery efficiency of MP-RDMA. Next, we let MP-RDMA's VPs randomly mapped onto the two parallel paths (denoted as MP-RDMA (Multi-path)), and evaluate whether MP-RDMA can avoid the bad paths. Both MELO and DCQCN are forced on the lossy path.

Fig. 25 shows the result. Benefited from SACK loss recovery, MELO can almost keep the maximal 40Gbps throughput under various loss rate. However, due to go-back-N loss recovery, current RDMA (DCQCN) can only achieve less than 50% throughput even under a very low loss rate (0.1%). Since we still use go-back-N loss recovery, throughput of MP-RDMA (Single-path) also drops to about 80% when encountering 0.1% loss. However, MP-RDMA (Single-path) behaves much better than DCQCN. It is because MP-RDMA receiver has a small bitmap to record OOO packets ($L = 64$ in our simulation) and OOO packets within the bitmap are buffered instead of simply dropped in DCQCN. Therefore, the sender can recover the loss more quickly. When there are multiple paths to use, MP-RDMA can quickly walk around the lossy path benefited from the OOO-aware path selection, and keeps almost the maximal 40Gbps throughput. The throughput is a little lower than MELO due to the overhead of packet header and the overhead during path selection/probing.

IX. CONCLUSION

This paper presents MP-RDMA, a multi-path transport for RDMA in datacenters. It can efficiently utilize the rich network paths in datacenters while keeping on-chip memory footprint low. MP-RDMA employs novel *multi-path ACK-clocking* and *out-of-order aware path selection* to choose best network paths and distribute packets among them in a congestion-aware manner. In total, MP-RDMA requires only a small constant (66B) amount of extra memory for each RDMA connection no matter how many network paths are used. Our FPGA-based prototype validates the feasibility for MP-RDMA's hardware implementation. Our evaluations on a small-scale testbed as well as large-scale simulation illustrate the effectiveness for MP-RDMA in utilizing the rich network paths diversity in datacenters.

ACKNOWLEDGMENT

The authors thank their NSDI shepherd M. Freedman and the anonymous reviewers for their valuable comments and suggestions. They thank D. Wei and T. Xu for their work on NS3 simulation for CONGA and MPTCP. They are grateful to W. Bai, R. Shu and H. Xu for their comments on the modeling. They also thank L. Luo for his discussion to improve the quality of the paper. Y. Wang, W. Xiao and S. Lee helped them to improve the writing.

REFERENCES

- [1] Y. Lu *et al.*, "Multi-path transport for RDMA in datacenters," in *Proc. 15th USENIX Conf. Netw. Syst. Design Implement.*, 2018, pp. 357–371.

- [2] Y. Zhu *et al.*, “Congestion control for large-scale RDMA deployments,” *ACM SIGCOMM Comput. Commun. Rev.*, vol. 45, no. 4, pp. 523–536, 2015.
- [3] C. Guo *et al.*, “RDMA over commodity Ethernet at scale,” in *Proc. ACM SIGCOMM Conf.*, 2016, pp. 202–215.
- [4] S. S. Vazhkudai *et al.*, “The design, deployment, and evaluation of the CORAL pre-exascale systems,” in *Proc. Int. Conf. High Perform. Comput., Netw., Storage, Anal.*, Piscataway, NJ, USA, 2018, p. 52.
- [5] C. Raiciu *et al.*, “Improving datacenter performance and robustness with multipath TCP,” in *Proc. ACM SIGCOMM Conf.*, New York, NY, USA, 2011, pp. 266–277.
- [6] M. Alizadeh *et al.*, “CONGA: Distributed congestion-aware load balancing for datacenters,” in *Proc. ACM Conf. SIGCOMM*, New York, NY, USA, 2014, pp. 503–514.
- [7] M. Al-Fares, S. Radhakrishnan, B. Raghavan, N. Huang, and A. Vahdat, “Hedera: Dynamic flow scheduling for data center networks,” in *Proc. 7th USENIX Conf. Netw. Syst. Design Implement.*, Berkeley, CA, USA, 2010, p. 19.
- [8] A. Kalia, M. Kaminsky, and D. G. Andersen, “Design guidelines for high performance RDMA systems,” in *Proc. USENIX Conf. Usenix Annu. Tech. Conf.*, 2016, pp. 437–450.
- [9] A. Kalia, M. Kaminsky, and D. G. Andersen, “FaSST: Fast, scalable and simple distributed transactions with two-sided (RDMA) datagram RPCs,” in *Proc. 12th USENIX Conf. Operating Syst. Design Implement.*, Savannah, GA, USA, 2016, pp. 185–201.
- [10] *Linux Cross Reference*. Accessed: Oct. 1, 2018. [Online]. Available: <http://lxr.free-electrons.com/source/include/linux/mlx4/qp.h>
- [11] C. Guo *et al.*, “Pingmesh: A large-scale system for data center network latency measurement and analysis,” *ACM SIGCOMM Comput. Commun. Rev.*, vol. 45, no. 4, pp. 139–152, 2015.
- [12] M. Wu *et al.*, “GraM: Scaling graph computation to the trillions,” in *Proc. 6th ACM Symp. Cloud Comput.*, 2015, pp. 408–421.
- [13] A. Dragojević, D. Narayanan, M. Castro, and O. Hodson, “FaRM: Fast remote memory,” in *Proc. 11th USENIX Conf. Netw. Syst. Design Implement.*, 2014, pp. 401–414.
- [14] B. F. Cooper, A. Silberstein, E. Tam, R. Ramakrishnan, and R. Sears, “Benchmarking cloud serving systems with YCSB,” in *Proc. 1st ACM Symp. Cloud Comput.*, Jun. 2010, pp. 143–154.
- [15] *InfiniBand Architecture Volume 1, General Specifications, Release 1.2.1*, Beaverton, OR, USA, InfiniBand Trade Association, 2008.
- [16] *InfiniBand Architecture Volume 2, Physical Specifications, Release 1.3*, Beaverton, OR, USA, InfiniBand Trade Association, 2012.
- [17] *Supplement to InfiniBand Architecture Specification Volume 1 Release 1.2.2 Annex A17: RoCEv2 (IP Routable RoCE)*, Beaverton, OR, USA, InfiniBand Trade Association, 2012.
- [18] R. Mittal *et al.*, “TIMELY: RTT-based congestion control for the datacenter,” *ACM SIGCOMM Comput. Commun. Rev.*, vol. 45, no. 4, pp. 537–550, 2015.
- [19] Cisco. *Priority Flow Control: Build Reliable Layer 2 Infrastructure*. Accessed: Oct. 1, 2018. [Online]. Available: http://www.cisco.com/en/US/prod/collateral/switches/ps9441/ps9670/white_paper_c11-542809_ns783_Networking_Solutions_White_Paper.html
- [20] *802.1Qbb—Priority-based Flow Control*. Accessed: Oct. 1, 2018. [Online]. Available: <http://www.ieee802.org/1/pages/802.1bb.html>
- [21] IEEE 802.1Qau Congestion NotificationNo. [Online]. Available: <http://www.ieee802.org/1/pages/802.1au.html>
- [22] G. Chen *et al.*, “Fast and cautious: Leveraging multi-path diversity for transport loss recovery in data centers,” in *Proc. USENIX Conf. Usenix Annu. Tech. Conf.*, 2016, pp. 29–42.
- [23] A. Singh *et al.*, “Jupiter rising: A decade of Clos topologies and centralized control in Google’s datacenter network,” *ACM SIGCOMM Comput. Commun. Rev.*, vol. 45, no. 4, pp. 183–197, 2015.
- [24] A. Roy, H. Zeng, J. Bagga, G. Porter, and C. A. Snoeren, “Inside the social network’s (datacenter) network,” *ACM SIGCOMM Comput. Commun. Rev.*, vol. 45, no. 4, pp. 123–137, 2015.
- [25] J. Cao *et al.*, “Per-packet load-balanced, low-latency routing for clos-based data center networks,” in *Proc. 9th ACM Conf. Emerg. Netw. Exp. Technol.*, New York, NY, USA, 2013, pp. 49–60.
- [26] M. Al-Fares, A. Loukissas, and A. Vahdat, “A scalable, commodity data center network architecture,” *ACM SIGCOMM Comput. Commun. Rev.*, vol. 38, no. 4, pp. 63–74, 2008.
- [27] A. Greenberg *et al.*, “VL2: A scalable and flexible data center network,” in *Proc. SIGCOMM*, 2009, pp. 51–62.
- [28] T. Benson, A. Anand, A. Akella, and M. Zhang, “MicroTE: Fine grained traffic engineering for data centers,” in *Proc. 7th Conf. Emerg. Netw. Exp. Technol.*, 2011, p. 8.
- [29] J. Rasley *et al.*, “Planck: Millisecond-scale monitoring and control for commodity networks,” *ACM SIGCOMM Comput. Commun. Rev.*, vol. 44, no. 4, pp. 407–418, 2015.
- [30] A. Dixit, P. Prakash, Y. C. Hu, and R. R. Komella, “On the impact of packet spraying in data center networks,” in *Proc. INFOCOM*, Apr. 2013, pp. 2130–2138.
- [31] J. Perry, A. Oosterhout, H. Balakrishnan, D. Shah, and H. Fugal, “Fast-pass: A centralized ‘zero-queue’ datacenter network,” *ACM SIGCOMM Comput. Commun. Rev.*, vol. 44, no. 4, pp. 307–318, 2014.
- [32] K. He, E. Rozner, K. Agarwal, W. Felter, J. Carter, and A. Akella, “Presto: Edge-based load balancing for fast datacenter networks,” *ACM SIGCOMM Comput. Commun. Rev.*, vol. 45, no. 4, pp. 465–478, 2015.
- [33] N. Katta *et al.*, “CLOVE: How I learned to stop worrying about the core and love the edge,” in *Proc. 15th ACM Workshop Hot Topics Netw.*, 2016, pp. 155–161.
- [34] S. Floyd and V. Jacobson, “Random early detection gateways for congestion avoidance,” *IEEE/ACM Trans. Netw.*, vol. 1, no. 4, pp. 397–413, Aug. 1993.
- [35] A. Gurto, T. Henderson, S. Floyd, and Y. Nishida, *The NewReno Modification to TCP’s Fast Recovery Algorithm*, document RFC 6582, RFC Editor, Apr. 2012. [Online]. Available: <https://rfc-editor.org/rfc/rfc6582.txt>; doi: [10.17487/RFC6582](https://doi.org/10.17487/RFC6582)
- [36] *ConnectX-5 EN IC*. Accessed: Oct. 1, 2018. [Online]. Available: http://www.mellanox.com/related-docs/prod_silicon/PB_ConnectX-5_EN_IC.pdf
- [37] A. Hughes, “Issues in TCP slow-start restart after idle,” Internet Eng. Task Force, Work Prog., Tech. Rep. draft-hughes-restart-00, Nov. 2001. [Online]. Available: <https://datatracker.ietf.org/doc/html/draft-hughes-restart-00>
- [38] *Ns3: A Discrete-Event Network Simulator for Internet Systems*. Accessed: Oct. 1, 2018. [Online]. Available: <https://www.nsnam.org/>
- [39] M. Alizadeh, A. Javanmard, and B. Prabhakar, “Analysis of DCTCP: Stability, convergence, and fairness,” in *Proc. ACM SIGMETRICS Joint Int. Conf. Meas. Modeling Comput. Syst.*, 2011, pp. 73–84.
- [40] Altera. *Stratix V FPGAs*. Accessed: Oct. 1, 2018. [Online]. Available: <https://www.altera.com/products/fpga/stratix-series/stratix-v/overview.html>
- [41] B. Li *et al.*, “ClickNP: Highly flexible and high performance network processing with reconfigurable hardware,” in *Proc. ACM SIGCOMM Conf.*, 2016, pp. 1–14.
- [42] Mellanox. *Connectx-3 Pro en Single/Dual-Port Adapters 10/40/56gbE Adapters W/ Pci Express 3.0*. Accessed: Oct. 1, 2018. [Online]. Available: http://www.mellanox.com/page/products_dyn?product_family=162&mtag=connectx_3_pro_en_card
- [43] Mellanox. *RoCE vs. iWARP Competitive Analysis*. Accessed: Oct. 1, 2018. [Online]. Available: http://www.mellanox.com/related-docs/whitepapers/WP_RoCE_vs_iWARP.pdf
- [44] Arista. *7050X & 7050X2 Switch Architecture ('A day in the life of a packet')*. Accessed: Oct. 1, 2018. [Online]. Available: https://www.arista.com/assets/data/pdf/Whitepapers/Arista_7050X_Switch_Architecture.pdf
- [45] Y. Lu *et al.*, “Memory efficient loss recovery for hardware-based transport in datacenter,” in *Proc. 1st Asia-Pacific Workshop Netw.*, 2017, pp. 22–28.
- [46] M. Alizadeh *et al.*, “Data center TCP (DCTCP),” in *Proc. ACM SIGCOMM Conf.*, New York, NY, USA, 2010, pp. 63–74.
- [47] R. Jain, A. Durresi, and G. Babic, “Throughput fairness index: An explanation,” Dept. Comput. Inf. Sci., The Ohio State University, Columbus, OH, USA, Tech. Rep. 99-0045, 1999.
- [48] S. Ghorbani, Z. Yang, P. B. Godfrey, Y. Ganjali, and A. Firoozshahian, “DRILL: Micro load balancing for low-latency data center networks,” in *Proc. Conf. ACM Special Interest Group Data Commun.*, New York, NY, USA, 2017, pp. 225–238.
- [49] E. Vanini, R. Pan, M. Alizadeh, P. Taheri, and T. Edsall, “Let it flow: Resilient asymmetric load balancing with flowlet switching,” in *Proc. 14th USENIX Conf. Netw. Syst. Design Implement.*, 2017, pp. 407–420.
- [50] Y. Cao, M. Xu, and X. Fu, “Delay-based congestion control for multipath TCP,” in *Proc. 20th IEEE Int. Conf. Netw. Protocols*, Oct./Nov. 2012, pp. 1–10.
- [51] Y. Cao, M. Xu, X. Fu, and E. Dong, “Explicit multipath congestion control for data center networks,” in *Proc. 9th ACM Conf. Emerg. Netw. Exp. Technol.*, 2013, pp. 73–84.
- [52] J. Anselmi and N. Walton, “Decentralized proportional load balancing,” *SIAM J. Appl. Math.*, vol. 76, no. 1, pp. 391–410, 2016.

- [53] Mellanox Technologies. *Multi-Path RDMA*. Accessed: Oct. 1, 2018. [Online]. Available: https://www.openfabrics.org/images/eventpresos/workshops2015/DevWorkshop/Tuesday/tuesday_04.pdf
- [54] *NS-3 Simulator for RDMA*. Accessed: Oct. 1, 2018. [Online]. Available: <https://github.com/bobzhuyb/ns3-rdma/>
- [55] R. Mittal *et al.*, “Revisiting network support for RDMA,” in *Proc. Conf. ACM Special Interest Group Data Commun.*, 2018, pp. 313–326.



Guo Chen received the Ph.D. degree from Tsinghua University in 2016. Before joining Hunan University, he was an Associate Researcher with Microsoft Research Asia from 2016 to 2018. He is currently an Associate Professor with Hunan University. His current research interests lie broadly in networked systems and with a special focus on data center networking.



Yuanwei Lu received the joint Ph.D. degree from the University of Science and Technology of China and Microsoft Research Asia in 2018. He is currently a Senior Software Engineer with Tencent. He is broadly interested in data center networking and networked systems.



Bojie Li received the Ph.D. degree in computer science from the University of Science and Technology of China (USTC) and Microsoft Research Asia (MSRA) in 2019. He was among the first to work on data center systems with programmable NICs. He is currently a Senior Developer with the Distributed and Parallel Software Lab, Central Software Institute, Huawei 2012 Labs.



Kun Tan is currently the Vice President of Central Software Institute, and the Director and a Chief Architect of Cloud Networking Lab, Huawei Technologies. He is a generalist in computer networking and communication, who has rich experience in all layers of computer networking from application layer to physical layer. He designed the Compound TCP (CTCP) protocol (shipped in Windows kernel) and invented the Sora software radio platform (publicly available from MSR).



Yongqiang Xiong received the B.S., M.S., and Ph.D. degrees in computer science from Tsinghua University, Beijing, China, in 1996, 1998, and 2001, respectively. He is currently a Lead Researcher with Microsoft Research Asia and leads the Networking Research Group. His research interests include computer networking and networked systems.



Peng Cheng received the B.S. degree in software engineering from Beihang University in 2010, and the Ph.D. degree in computer science and technology from Tsinghua University in 2015. He was a Visiting Student with UCLA from September 2013 to September 2014. He is currently a Researcher with Microsoft Research Asia. His research interests are computer networking and networked systems and with a recent focus on data center networks.



Jiansong Zhang received the bachelor’s and master’s degrees from Tsinghua University and the Ph.D. degree from The Hong Kong University of Science and Technology. He was a Researcher with Microsoft Research Asia. He is currently a Staff Engineer with Alibaba Group. He has published tens of articles in Sigcomm, NSDI, Mobicom, Ubicomp, Mobisys, HotNets, and HotChips. His research interests are building innovative software and hardware systems.



Thomas Moscibroda received the Ph.D. degree from ETH Zurich in Switzerland, in 2006, and was awarded the ETH Medal for his doctoral thesis. He is currently a Partner Research Scientist with Microsoft Azure. In this role, he is driving and overseeing projects aimed at increasing Microsoft’s cloud computing efficiency, and cloud capacity experience. Many of his cloud resource management technologies have become core infrastructure components in Microsoft Azure data centers. Before joining Azure in September 2017, he managed the Cloud & Mobile Research Group, Microsoft Research Asia. He was also the Chair Professor for Network Science with the Institute for Interdisciplinary Information Sciences (IIIS), Tsinghua University. Before moving to China in 2011, he was a member of the Systems Research Group at Microsoft Research in Redmond, and an affiliate member of the Networking Research and Computer Architecture Research groups, respectively.